Adsorption of Cu, Cd, Zn and Pb Ions from Aqueous Solutions by Electric Arc Furnace Slag and the Effects of pH and Grain Size

X. Chen,[b] W. H. Hou,[a,*] G. L. Song,[c] and Q. H. Wang[d]

[a]Research Center of Water Pollution Control Technology, Chinese Research Academy of Environment Sciences, Beijing 100012, China

[b]Department of Municipal Engineering, Shandong Urban&Rural Planning Design Institute, Jinan 250013, China

[c]Department of Life Science, Shandong University of Technology, Zibo 255049, China

[d]Department of Environmental Engineering, University of Science and Technology Beijing, Beijing 100083, China

Original scientific paper
Received: July 31, 2009
Accepted: February 15, 2011

The study was carried out to investigate the adsorption kinetics and equilibrium of four heavy metal ions (Cu^{2+}, Cd^{2+}, Zn^{2+} and Pb^{2+}) on two kinds of electric arc furnace slag (EAF slag). The adsorption capacity of the Shougang slag (SG slag) is more than that of the Baoshan slag (BS slag). The metal adsorption on the EAF slag is more akin to the first-order kinetic model. Experimental data confirmed that Freundlich model was better in describing the metal adsorption on SG slag, while Langmuir model was more applicable for BS slag. The adsorption of metal ions increased with the pH value and reached a maximum at a 7 value for the Zn^{2+} and Pb^{2+} adsorption on SG slag. The decrease of grain size could enhance the adsorption of metal ions. The results established the potential use of EAF slag as costly adsorbents for heavy metal from contaminated wastewaters.

Key words:
EAF slag, heavy metal ions, adsorption, pH, grain size

Introduction

Over the past few decades, various heavy metals have been released into terrestrial and aquatic ecosystems due to their increased use in metal processing, electroplating, ceramic and glass production, mining operations, tanneries, and battery manufacture.[1,2] The increasing environmental contamination with heavy metal ions has become a great concern for ecological systems, public residing and human health, due to their toxicity, accumulation in food chain, and persistence in nature.[3] Environmental contamination by these metals is mainly due to the discharge of industrial wastewaters; therefore most researchers focus on cost-effective alternative technologies for removal or recovery of metals from contaminated waste streams. A great number of technologies are available for removal of heavy metals from solution, including ion exchange, reversed osmosis, membrane separation, and ultrafiltration.[4] However, these processes have considerable drawbacks, such as incomplete metal removal, generation of toxic sludge requiring advanced disposal process, and especially high operating cost.[5] In recent years, adsorption and fluidized-bed reactors have been regarded as more cost effective solutions than those classical techniques,[6,7] and more attention has been paid to the investigation of low-cost adsorbents such as industrial wastes, agricultural byproducts, and bio-materials for the removal of heavy metal ions from industrial wastewater. The low-cost materials reported in previous study included soybean straw,[1] arca shell biomass,[3] sewage sludge,[8] natural zeolite and zeolite synthesized from coal fly ash,[9,10] alkaline industrial residues,[11] olive pomace,[12] marine green alga *Ulva reticulate*,[13] and black gram husk,[14] et al.

Slag has also been reported as potential adsorbents to remove heavy metals from wastewater. Slag is the final waste from the iron and steel industry. There are three types of steel industry slag, namely blast furnace (BF) iron slag, basic oxygen furnace (BOF) steel slag, and electric arc furnace (EAF) steel slag.[15,16] Slag is used as fill material in road construction, phosphate fertilizer, and low-cost adsorbent in water and wastewater treatment instead of activated carbon.[17] Many studies have been conducted to investigate the potency of slag to remove phosphorus, dye and organic matter from wastewaters.[16–19] However, few studies

*Corresponding author: Email address: houwenhuahit@sina.com; xchen82@hotmail.com

have been reported on the removal of heavy metal ions from aqueous solutions using slag and little is known about the influence of solution pH and grain size on the performance of slag in wastewater treatment.[20,21] In the present study, Cu^{2+}, Cd^{2+}, Zn^{2+} and Pb^{2+} were selected as target heavy metals. The objectives of the study are as follows: (1) determine the adsorption kinetics and equilibrium of four heavy metal ions Cu^{2+}, Cd^{2+}, Zn^{2+} and Pb^{2+} on two EAF slags; (2) evaluate the effects of pH and grain size on metal uptake by EAF slag; and (3) determine the adsorption mechanisms of metals on the EAF slag.

Materials and methods

Materials

The material used in this study was electric arc furnace (EAF) steel slag. During the steelmaking process, iron ore and steel scrap were melted in the furnace along with fluxing agent (mainly lime) and molten impurities of steel. After the slag was cooled and solidified, the nonmetallic slag was removed and sized.[15,16] The two EAF slags were obtained from Baoshan Iron Steel factory (Shanghai, China) and Shougang factory (Beijing, China), namely BS slag and SG slag. The selected physico-chemical characteristics of the two slags are given in Table 1. The chemical analysis of slag was carried out with ICP-AES following a standard digestion method. The BET surface area was determined with Quantachrome Nova 3200e surface area analyzer. The pH value of the materials was measured using a pH meter in a 1 : 2.5 (w/v) substrate/water mixture after equilibrating for 30 min. The mineralogical compositions was determined by X-ray diffraction (XRD, Philips X'pert PRO) with Cu-Kα radiation of λ = 0.154 nm, 40 kV, 30 mA and the surface microstructure was observed by the scanning electron microscopy (SEM, JSM-6700F).

Batch adsorption experiments

Stock heavy metal solutions containing 20 mmol L^{-1} were separately prepared by dissolving appropriate amounts of $Cu(NO_3)_2 \cdot 3H_2O$, $Cd(NO_3)_2 \cdot 4H_2O$, $Zn(NO_3)_2 \cdot 6H_2O$, $Pb(NO_3)_2$ in double-distilled water and used to prepare the adsorbate solutions of the required concentrations.

The mechanical faction of the two EAF slags (BS slag and SG slag, 0.90~2.00 mm) was used in the adsorption kinetics study. Three replicates of air-dried slag (2 g) were placed in 250 mL Erlenmeyer flasks containing 200 mL heavy metal ion solution with initial concentration 2 mmol L^{-1}. The background ionic strength was adjusted to 5 mmol L^{-1} with $NaNO_3$. The initial pH of the solution was 5.0 and the temperature of the solutions was controlled at 25 °C Then each flask was capped and shaken at 180 rpm in rotary shaking incubator. Solution samples were taken periodically at 0.5 to 24 h and then metal concentrations in the filtered aqueous phases were determined by atomic absorption spectrometry (AAS) (Shimadzu, AA-6300).

In batch equilibrium study, three replicates of the two slags (0.5 g, 0.90~2.00 mm) were shaken with 50 mL heavy metal solution of different initial concentration (0.2, 0.4, 0.8, 1.2, 1.6, 2, 2.4 and 3.2 mmol L^{-1}) (180 rpm, 25 °C). The initial pH and temperature of solutions were kept at 5 and 25 °C. Then the solution was shaken at 180 rpm. After 24 h the solution containing heavy metal ions was filtrated and analyzed.

For SG EAF slag, adsorption equilibrium and kinetics experiments were performed with different mechanical factions (2.00~4.00 and 0.45~0.90 mm) to study the effects of grain size. To study the effects of pH on adsorption of heavy metal ions, three replicates of BS slag and SG slag (0.5 g, 0.90~2.00 mm) were placed with 50 mL solutions containing heavy metal ions (2 mmol L^{-1}) with different initial pH (2, 3, 4, 5, 6, 7 and 8). The flasks were shaken at 180 rpm in incubator for 24 h and then solutions were filtrated and analyzed.

Adsorption theory description

The kinetics of metal adsorption was modeled applying the first- and second-order kinetics models expressed as eqs. (1) and (2),[22] respectively:

First-order kinetics model:

$$q = q_e(1 - e^{-k_1 t}) \quad (1)$$

where q_e and q are the amount of solute adsorbed (mmol g^{-1}) at equilibrium and time t (min), respectively, and k_1 is the rate constant of the first-order adsorption (min^{-1}).

Table 1 – *Chemical and physical characteristics of the two EAF slags*

Material (0.90~2.00 mm)	Chemical composition, *w*/%						BET surface area/m^2 g^{-1}	Density/ g cm^{-3}	pH
	Ca	Mg	Al	Fe	Mn	Si			
BS slag	30.88	5.80	2.85	20.80	2.62	6.25	3.418	3.096	10.69
SG slag	36.63	9.04	0.67	15.05	1.02	7.08	0.445	3.974	11.75

Second-order kinetics model:

$$q = \frac{q_e^2 k_2 t}{1 + q_e k_2 t} \tag{2}$$

where k_2 is the rate constant of the second-order adsorption (mmol g^{-1} min^{-1}).

The adsorption isotherm was tested with respect to the following models:[23]

Freundlich model:

$$Q = K_F c_e^{1/n} \tag{3}$$

where Q is equilibrium metal concentration on adsorbent (mmol g^{-1}), c_e is the equilibrium concentration of metal ions in solution (mmol L^{-1}), K_F and n are Freundlich adsorption constants.

Langmuir model:

$$Q = \frac{Q_{\max} K_L c_e}{1 + K_L c_e} \tag{4}$$

where Q is equilibrium metal concentration on adsorbent (mmol g^{-1}), c_e is the equilibrium concentration of metal ions in solution (mmol L^{-1}), Q_{max} is the adsoption capacity (mmol g^{-1}) and K_L is Langmuir adsorption constant (L $mmol^{-1}$). The non-linear curve fitting of the models was conducted using software SPSS13. The goodness of fit of the models to experimental data was checked by comparison of the correlation coefficient R^2.

Results and discussion

Chemical and physical characteristics of the two EAF slags

Table 1 lists the chemical and physical characteristics of the two EAF slags. The result showed that the EAF slag was rich in Ca and Fe. For other elements, content of Mg and Si was relatively high. Compared with BS slag, SG slag has higher Ca content and lower Fe content, representing 36.63 % and 15.05 %, respectively. BS slag had greater BET surface area (3.418 m^2 g^{-1}), which meant BS slag might have more sorption sites. The density (3.974 g cm^{-3}) and pH (11.75) of SG slag was higher than those of BS slag. XRD was used to analyze the compounds phase present in the EAF slag. As shown in Fig. 1, the crystal compounds detected in EAF slag could be attributed to Brownmillerite ($Ca_2Fe_{1.4}Mg_{0.3}Si_{0.3}O_5$), Wuestite (FeO), Larnite (Ca_2SiO_4). XRD analysis confirmed the slag mainly consisted of metal oxide in various oxide and silicate form. Fig. 2 shows the SEM photographs of the two EAF slags. The SEM images

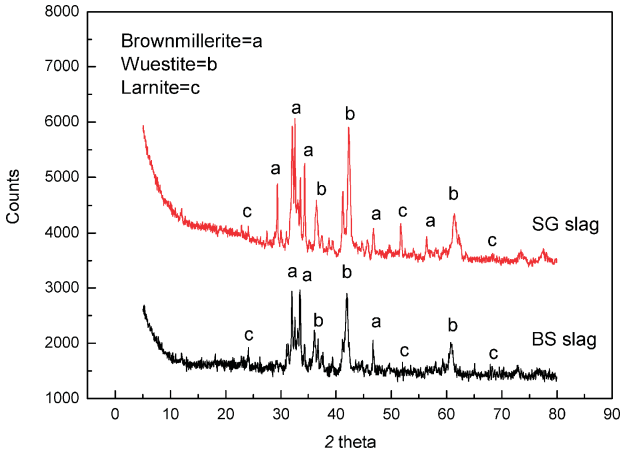

F i g . 1 – *XRD analysis of the two EAF slags*

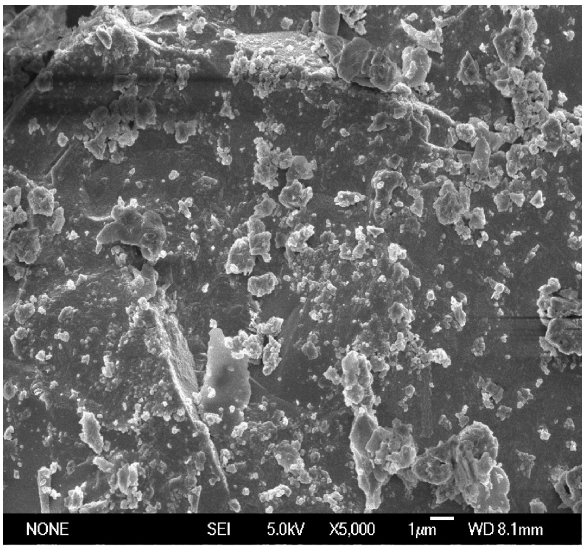

BS slag

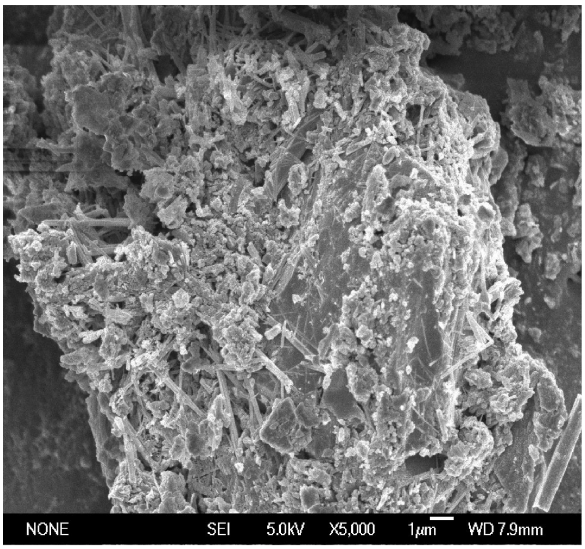

SG slag

F i g . 2 – *SEM photographs of the two EAF slags*

show the morphological differences between the BS slag and SG slag. BS slag had more complex surface structures, which is different from the smooth surface of the SG slag. The morphological structure of BS slag resulted in the higher BET surface area which was about 8 times of that of SG slag.

Adsorption kinetics of metal ions on the two EAF slags

Fig. 3 shows the adsorption kinetics of heavy metal ions (Cu^{2+}, Cd^{2+}, Zn^{2+}, Pb^{2+}) from aqueous solutions onto the two EAF slags (0.90~2.00 mm). For BS slag, the adsorption rate of heavy metal ions was very high in the early hours of the sorption experiments, as a large number of adsorption sites were available for adsorption at the start of the process. As the sites were gradually filled up, the kinetics became more dependent on the rate at which the adsorptive was transported from the bulk phase to the actual adsorption sites.[24] As shown that the adsorption of metal ions on BS slag approached equilibrium after about 300 min, and with the initial concentration of 2 mmol L^{-1} in aqueous solution, the equilibrium adsorption of metal ions was about 0.1 mmol g^{-1}. It could be seen that apparent differences of adsorption kinetics of heavy metal ions existed between the two EAF slags. For SG slag, the uptake rate for heavy metal ions at the initial periods was lower than that of BS slag and it took much more time (about 600~900 min) to achieve equilibrium process. However, the equilibrium adsorption of metal ions on BS slag was much higher than that of SG slag, and it could reach as high as 0.15 mmol g^{-1}.

In our opinion the noted differentiation of adsorption kinetics between the two slags was conditioned mainly by the different surface structures of the slag. According to Table 1, the BET surface area of BS slag was 3.418 m^2 g^{-1}, which was about 8 times that of the SG slag. Thus, BS slag had more pores available for metal adsorption and metal ions could occupy the adsorption sites more easily.

To better understand the adsorption kinetics, the non-linear curve fittings were conducted using SPSS software. The kinetic parameters obtained from model simulations are given in Table 2. Fig. 3 also presents the comparison of the first-order and second-order kinetic models with the experimental

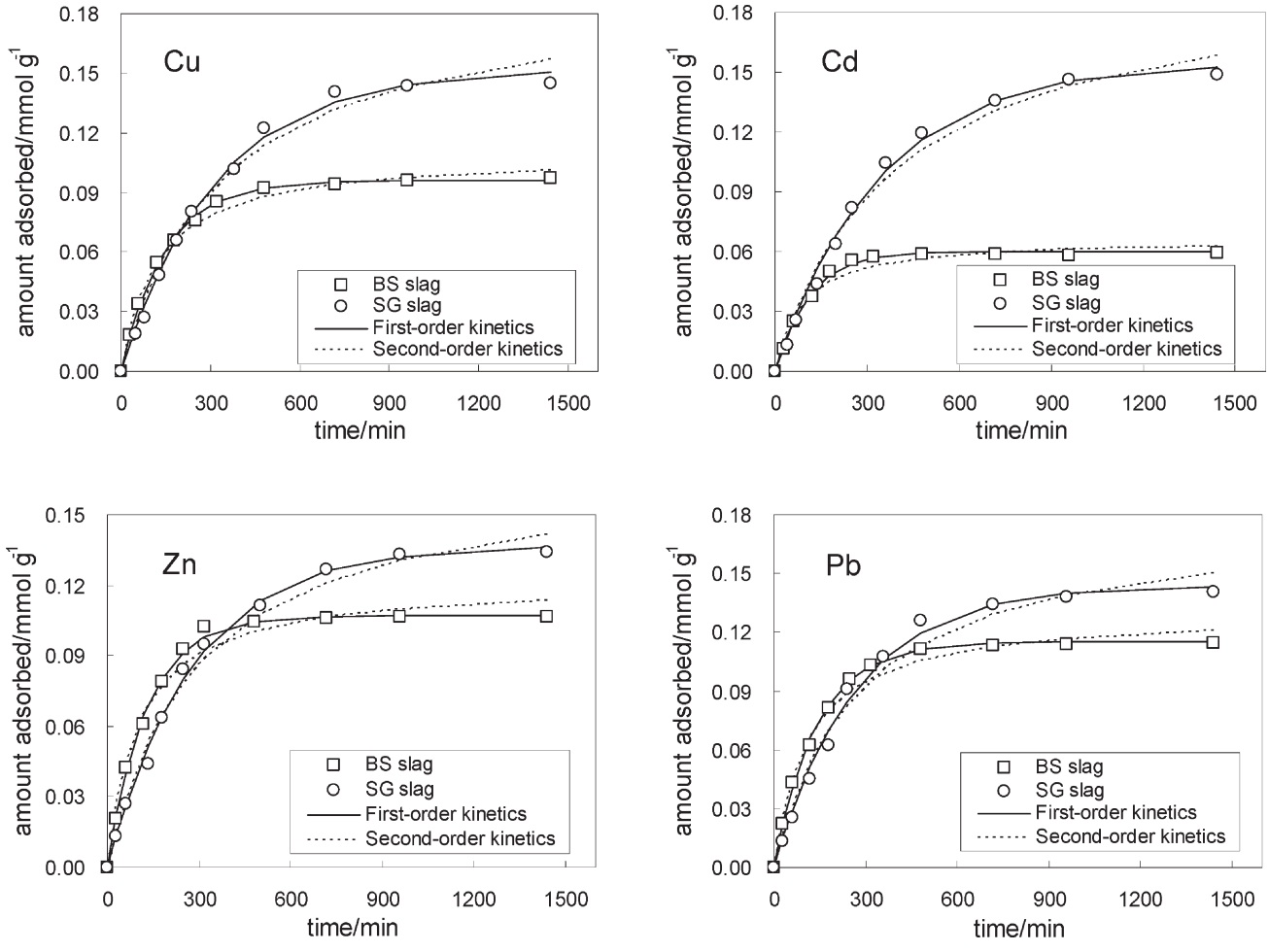

Fig. 3 – *Adsorption kinetics of metal ions on the EAF slag*

Table 2 – *Parameters of kinetics models for metal adsorption on the EAF slag*

Ions	Adsorbent	First-order kinetics			Second-order kinetics		
		q_e	k_1	R^2	q_e	k_2	R^2
Cu	BS slag	0.096	0.0068	0.998	0.110	0.077	0.992
	SG slag	0.152	0.0031	0.995	0.195	0.015	0.983
Cd	BS slag	0.060	0.0091	0.994	0.067	0.177	0.966
	SG slag	0.155	0.0029	0.995	0.201	0.013	0.986
Zn	BS slag	0.107	0.0077	0.997	0.122	0.081	0.980
	SG slag	0.137	0.0035	0.996	0.171	0.020	0.989
Pb	BS slag	0.115	0.0071	0.997	0.131	0.068	0.977
	SG slag	0.145	0.0036	0.993	0.181	0.020	0.979

data for BS slag and SG slag. Both first-order and second-order kinetics gave good fit to the experimental data (R^2∼0.966 to 0.998). Compared with the experimental equilibrium adsorption, the first-order kinetics produced better fitting results in terms of correlation coefficient (R^2∼0.993 to 0.998), which suggests that the adsorption kinetics of four metals on the two EAF slags followed the first-order kinetic model. However, Nehrenheim and Gustafsson investigated the kinetics of heavy metal ions (Cu^{2+}, Zn^{2+}, Pb^{2+}) removal by the use of EAF slag and reported to be the second-order kinetics.[25] The differences of adsorption kinetics between various EAF slags mainly attributed to different physico-chemical characteristics or surface structures.[1,24] Moreover, the amount of heavy metal ions uptake by SG slag (0.137~0.155 mmol g^{-1}) was higher than that of BS slag (0.060~0.115 mmol g^{-1}).

Adsorption equilibrium of metal ions on the two EAF slag

Fig. 4 illustrates the adsorption isotherm of four heavy metal ions on the EAF slag (0.90~2.00 mm). The equilibrium adsorption Q increased with the increase in metal concentration in the solution. Comparing the two isotherms, metal adsorption of SG slag was higher than that of BS slag, especially for Cd. For SG slag, equilibrium adsorption approached 0.15 mmol g^{-1} when equilibrium concentration was over 5 mmol L^{-1}, whereas the uptake of metals on BS slag was much lower with an adsorption capacity of about 0.1 mmol g^{-1}. Freundlich and Langmuir isotherm model was employed to describe the metal

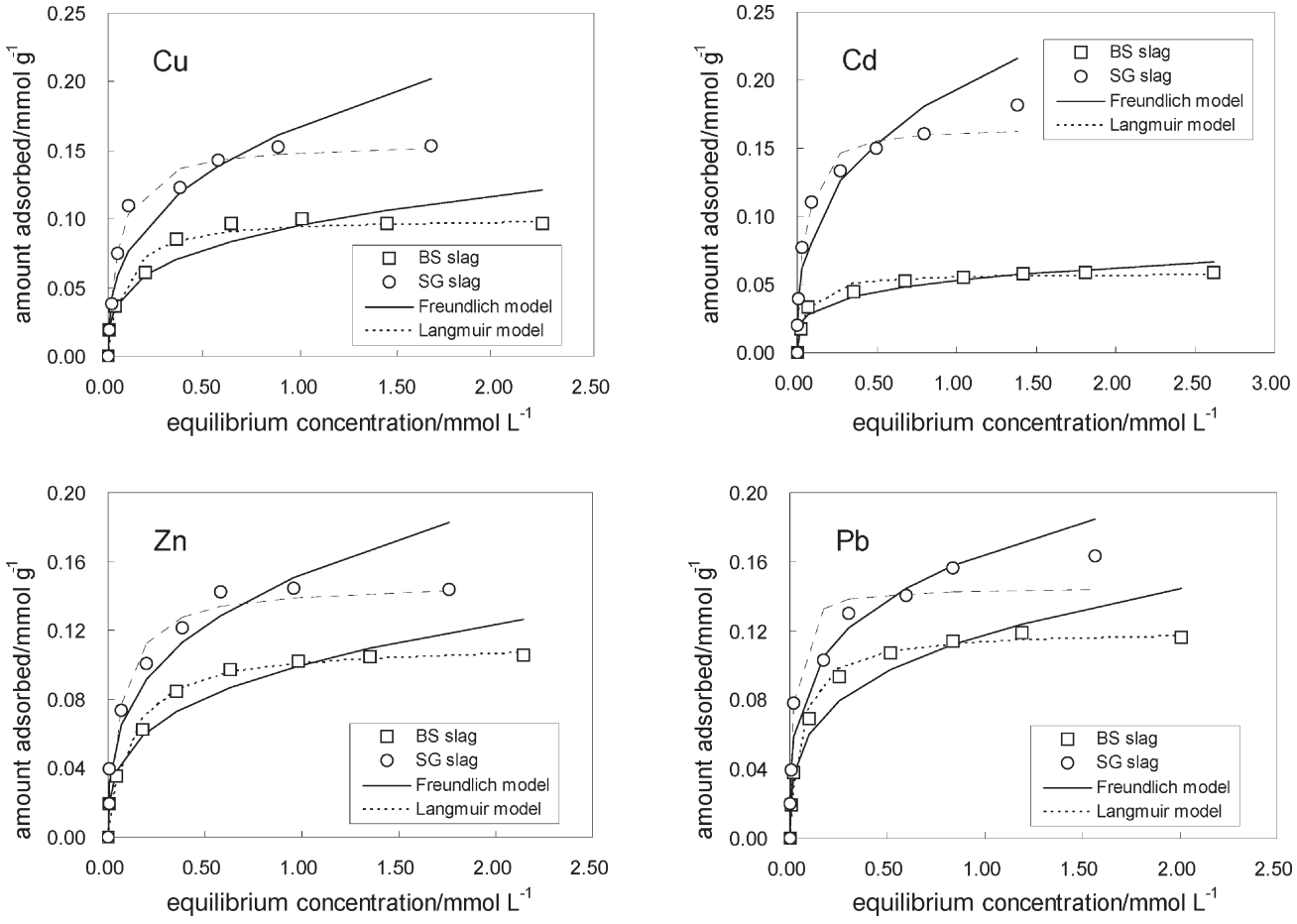

Fig. 4 – *Adsorption isotherms of Cu, Cd, Zn and Pb ions on the EAF slag*

adsorption by the EAF slag. The parameters of two isotherms calculated with eqs. are presented in Table 3 and the fitting curves to the experimental data are shown in Fig. 4. Comparison of the correlation coefficients and fitting curves produced by the two models revealed that Langmuir model was more applicable for the BS slag adsorption of four heavy metal ions. While for SG slag, Langmuir model fitted better for the sorption of Cu^{2+} and Zn^{2+}, and Freudlich model was better in describing Cd^{2+} and Pb^{2+} isotherms.

Table 3 – *Parameters of isotherm models for metal adsorption on the EAF slag*

Ions	Adsorbent	Freundlich model			Langmuir model		
		K_F	$1/n$	R^2	Q_{max}	K_L	R^2
Cu	BS slag	0.096	0.292	0.946	0.101	13.493	0.949
	SG slag	0.169	0.348	0.917	0.156	19.305	0.982
Cd	BS slag	0.053	0.233	0.921	0.058	19.024	0.967
	SG slag	0.190	0.312	0.962	0.166	28.444	0.957
Zn	BS slag	0.100	0.306	0.970	0.112	9.235	0.966
	SG slag	0.153	0.315	0.931	0.148	16.199	0.941
Pb	BS slag	0.118	0.289	0.962	0.120	17.675	0.963
	SG slag	0.165	0.255	0.968	0.145	66.539	0.905

Langmuir theory concerns sorption onto materials of homogeneous specific surfaces and involves monolayer chemisorption. Therefore, a maximum adsorption capacity Q_{max} can be obtained from the fittings of adsorption isotherm. The Q_{max} values for Cu^{2+}, Cd^{2+}, Zn^{2+}, Pb^{2+} adsorption on BS slag were 0.101, 0.058, 0.112, 0.120 mmol g^{-1} and those for SG slag are 0.156, 0.166, 0.148, 0.145 mmol g^{-1} in the same order of metal ions. Curkovic *et al*. conducted experiment to obtain the adsorption capacities of Cu^{2+} and Pb^{2+} on EAF slag at 30 °C.[21] The adsorption capacities by Langmuir model of Cu^{2+} and Pb^{2+} were 36.36 and 35.84 mg g^{-1}, respectively. Other studies rarely reported the adsorption capacity of heavy metal ions on EAF slag.[20,25]

The sorption capacity for metals by BS slag followed the order $Pb^{2+} > Zn^{2+} > Cu^{2+} > Cd^{2+}$ while the order for SG slag follows $Cd^{2+} > Cu^{2+} > Zn^{2+} > Pb^{2+}$. The most evident disparity could be observed in the adsorption capacity of Cd^{2+} between the BS slag and SG slag. To our thinking, the noted increase of Cd^{2+} adsorption by SG slag was mainly attributed to the formation of metal hydroxides. Table 1 shows that pH value of SG slag was higher than that of BS slag. And the order of the K_{sp} values of the four heavy metal ions was $Cd(OH)_2 < Pd(OH)_2 < Cu(OH)_2 < Zn(OH)_2$, the corresponding values being $3.6 \cdot 10^{-29}$, $1.42 \cdot 10^{-20}$, $2.2 \cdot 10^{-20}$ and $1.8 \cdot 10^{-14}$, respectively. Consequently, as the pH of aqueous solutions increased, more Cd^{2+} ions could be removed.

The metal uptake of EAF slag is attributed to different mechanisms of containing physorption and chemisorption, ion exchange, surface precipitation. According to results of the adsorption experiment and previous study,[20,21] possible mechanisms can be presented as follows:

$$(Al,Si-O)_2^-Ca^{2+} + 2H_2O \Leftrightarrow \Leftrightarrow 2(Al,Si-O)^-H^+ + Ca^{2+} + 2OH^- \quad (5)$$

$$2(Al,Si-O)^-H^+ + Me^{2+} \Leftrightarrow \Leftrightarrow (Al,Si-O)_2^-Me^{2+} + 2H^+ \quad (6)$$

$$(Al,Si-O)_2^-Ca^{2+} + Me^{2+} \Leftrightarrow \Leftrightarrow (Al,Si-O)_2^-Me^{2+} + Ca^{2+} \quad (7)$$

$$(Al,Si-O)_2^-Ca^{2+} + 2MeOH^+ \Leftrightarrow \Leftrightarrow 2(Al,Si-O)^-MeOH^+ + Ca^{2+} \quad (8)$$

$$Me^{2+} + 2OH^- \Leftrightarrow 2Me(OH)_2 \downarrow \quad (9)$$

The BET surface area of BS slag was 8 times that of SG slag. Assuming that the surface of two EAF slag grain was of same structure, the adsorption capacity Q_{max} for metal ions of BS slag should be more than that of SG slag. In fact, results were contrary to expectations. Moreover, many precipitates could be observed at the end of adsorption experiment with SG slag and such phenomena did not occur in the experiment with BS slag. The collected precipitates were freeze dried and analyzed with XRD (Fig. 5). The XRD analysis confirmed that the precipitates were mainly heavy metal ions hydroxide. Therefore, it can be concluded that the mechanism of heavy metal ions adsorption on BS slag is different from SG slag. For BS slag, the mechanisms involved rapid adsorption and ion exchange (shown as reaction (7), (8)). Metal ions moved through the pores of the BS slag and they replaced exchangeable cations (mainly Ca^{2+}) and additionally exchanged with protons of surface hydroxyl groups. While mechanisms for metal removal by SG slag was relatively complicated. It could be attributed to different mechanisms of physorption and chemisorption, ion exchange, surface precipitation. At the initial stage, quick adsorption and ion exchange occurred just like BS slag. Then the hydrolysis of SG slag and precipitation kinetics took place shown as reaction (5) and (9), the rate of

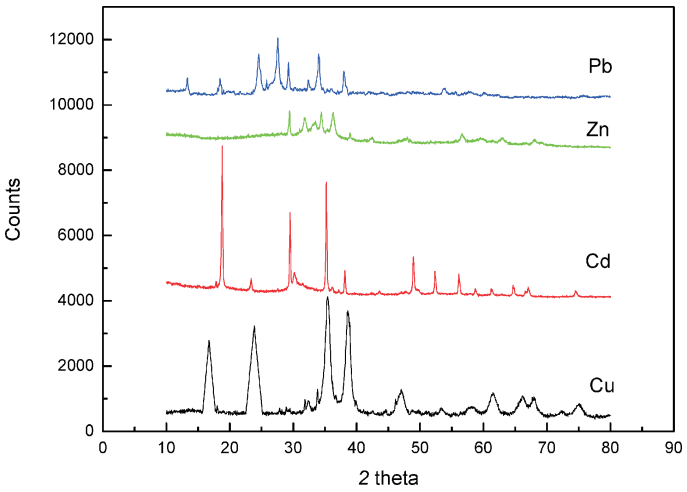

Fig. 5 – *XRD analysis of metal precipitates deposited on SG slag*

which was much slower than adsorption or exchange kinetics. As a result, it took more time for the sorption of metal ions on SG slag to achieve equilibrium process compared with BS slag, which could be proved by Fig. 3.

Effect of pH on metal ions adsorption

The pH level of aqueous solution is an important variable for the adsorption of metal ions on the adsorbents. Fig. 6 presents the variation of metal adsorption on EAF slag at varying solution pH. For BS slag, the adsorption of the four metals (Cu^{2+}, Cd^{2+}, Zn^{2+}, Pb^{2+}) increased with the increasing pH. For SG slag, the effect of pH was exactly the same when the pH was in the range of 2 to 7. However, when the pH increased from 7 to 8, the adsorption of Zn^{2+} and Pb^{2+} on SG slag slightly decreased.

The results can be explained from two aspects. Firstly, as the pH level increases, the concentration of the hydrogen ions acting as competitors decreases, which leads to an increase of the amounts of sorbed metals. Secondly, heavy metal ions will react with hydroxyl species in aqueous solution, forming various species (such as $Me(OH)^+$, $Me(OH)_2$). When pH is increased, more hydroxyl ion will be presented in the solution, resulting in surface precipitation. However, things seemed different for the sorption of Zn^{2+} and Pb^{2+} by SG slag when the initial pH of solutions increased from 7 to 8. As is well known, $Zn(OH)_2$ and $Pb(OH)_2$ were amphoteric hydroxide, and therefore at higher pH level the hydroxide became dissolved. For the metal sorption by SG slag, large amounts of metal precipitates existed in the solution. When the pH was too high, the metal deposits ($Zn(OH)_2$ and $Pb(OH)_2$) would become dissolved and therefore the removal efficiency decreased.

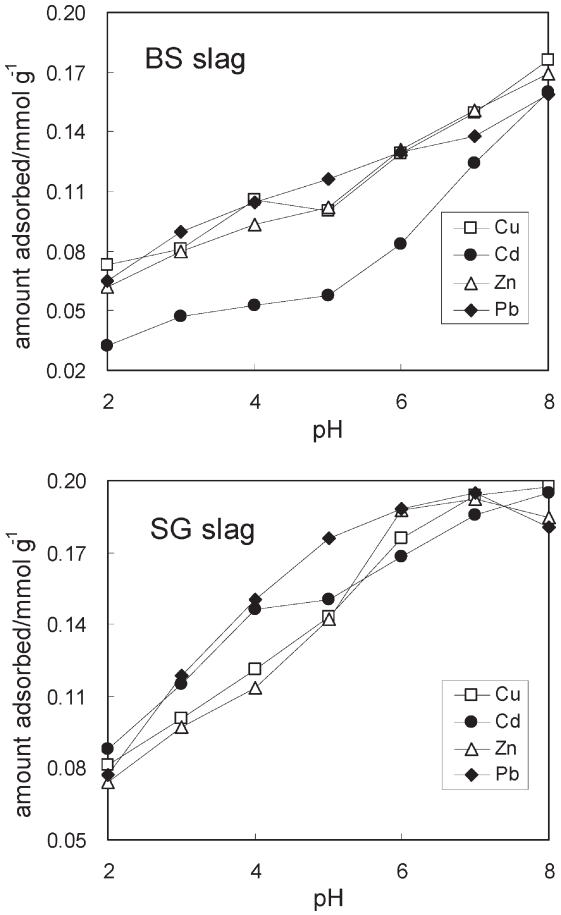

Fig. 6 – *Effects of pH on heavy metal adsorption on EAF slag*

Effect of grain size on metal ions adsorption

Experiments performed with initial concentration of 2 mmol L^{-1} documented the effects of slag grain size on the adsorption kinetics of metal ions (Fig. 7). As expected, as the grain size decreased the adsorption rate of metal ions increased progressively. After 24 h, the adsorption did not reach equilibrium in the experiments performed with the larger grain size (2.00∼4.00 mm), while equilibrium had already been achieved in those performed with smaller grain size. The specific surface area of the SG slag (0.90∼2.00 mm) was only 0.445 $m^2\,g^{-1}$ and SG slag did not have much porous structure. The decrease of the grain size of slag would increase sites available for metal sorption and hence improved accessibility of metal diffusion flows to adsorption centers. On the other hand, the decrease of particle size would increase high rates of the ion exchange process according to the theory.[26] The results were in agreement with the adsorption of heavy metal ions on agrogonite shells and clinoptilolite.[2,27] However, Ouki and Wingenfelder found that the sizes of zeolite grains had no influence on

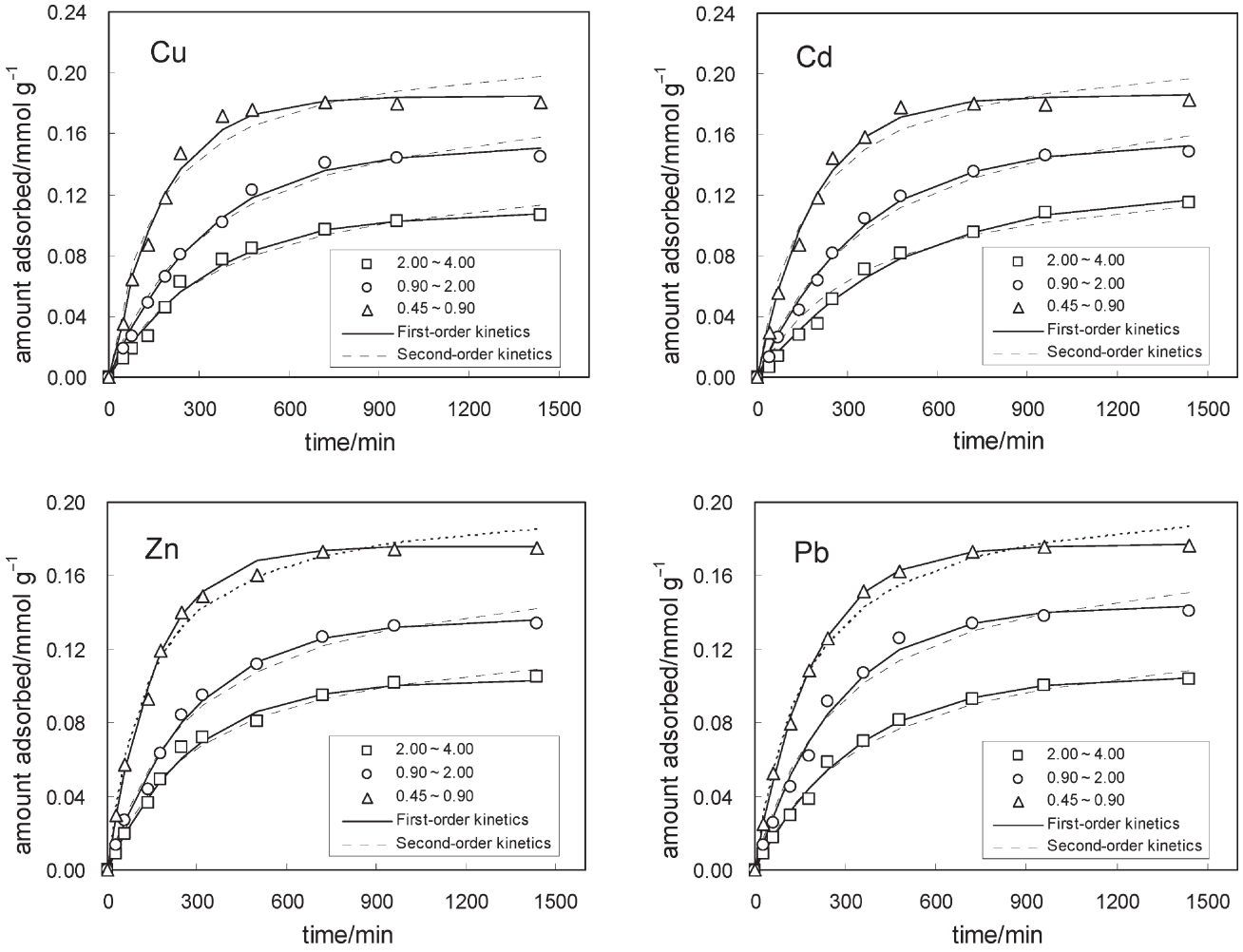

Fig. 7 – *Adsorption kinetics of metal ions on SG slag of different grain size*

sorption efficiency because the process does not occur on the grain's surface but in the porous void.[28,29] Furthermore, the study by Zorpas et al. pointed out that the decrease of grain size resulted in poor uptake of heavy metal ions by clinoptilolite, since the grinding process to achieve fine particles would result in the damage of pore structures and the decrease of the BET surface area.[26] According to the experimental results, the decrease of grain size of SG slag would enhance the uptake of heavy metal ions in the batch adsorption, while the effects of grain size on metal removal efficiency in practical column experiments need consideration. Too fine grain size may cause column clogging and decrease metal removal efficiency.

The adsorption isotherms of heavy metal ions on SG slag with different grain size are presented in Fig. 8. Table 4 illustrates the effects of grain size on the parameters of isotherm models for metal adsorption. It was observed that as the grain size of SG slag decreased from 2.00∼4.00 mm to 0.45∼0.90 mm, the adsorption capacity Q_{max} of four metals increased by about 100 %. Comparison of the

Table 4 – *Parameters of isotherm models for metal adsorption on SG slag of different grain size*

Ions	Size range	Freundlich model			Langmuir model		
		K_F	1/n	R^2	Q_{max}	K_L	R^2
Cu	2.00∼4.00	0.111	0.291	0.914	0.113	20.999	0.961
	0.90∼2.00	0.169	0.348	0.917	0.156	19.305	0.982
	0.45∼0.90	0.303	0.393	0.974	0.232	18.416	0.971
Cd	2.00∼4.00	0.134	0.258	0.890	0.125	46.805	0.979
	0.90∼2.00	0.190	0.312	0.962	0.166	28.444	0.957
	0.45∼0.90	0.331	0.346	0.962	0.224	42.134	0.901
Zn	2.00∼4.00	0.109	0.248	0.908	0.105	55.296	0.908
	0.90∼2.00	0.153	0.315	0.931	0.148	16.199	0.941
	0.45∼0.90	0.244	0.325	0.969	0.219	14.181	0.929
Pb	2.00∼4.00	0.118	0.230	0.934	0.111	68.268	0.946
	0.90∼2.00	0.165	0.255	0.968	0.145	66.539	0.905
	0.45∼0.90	0.278	0.313	0.977	0.215	31.164	0.903

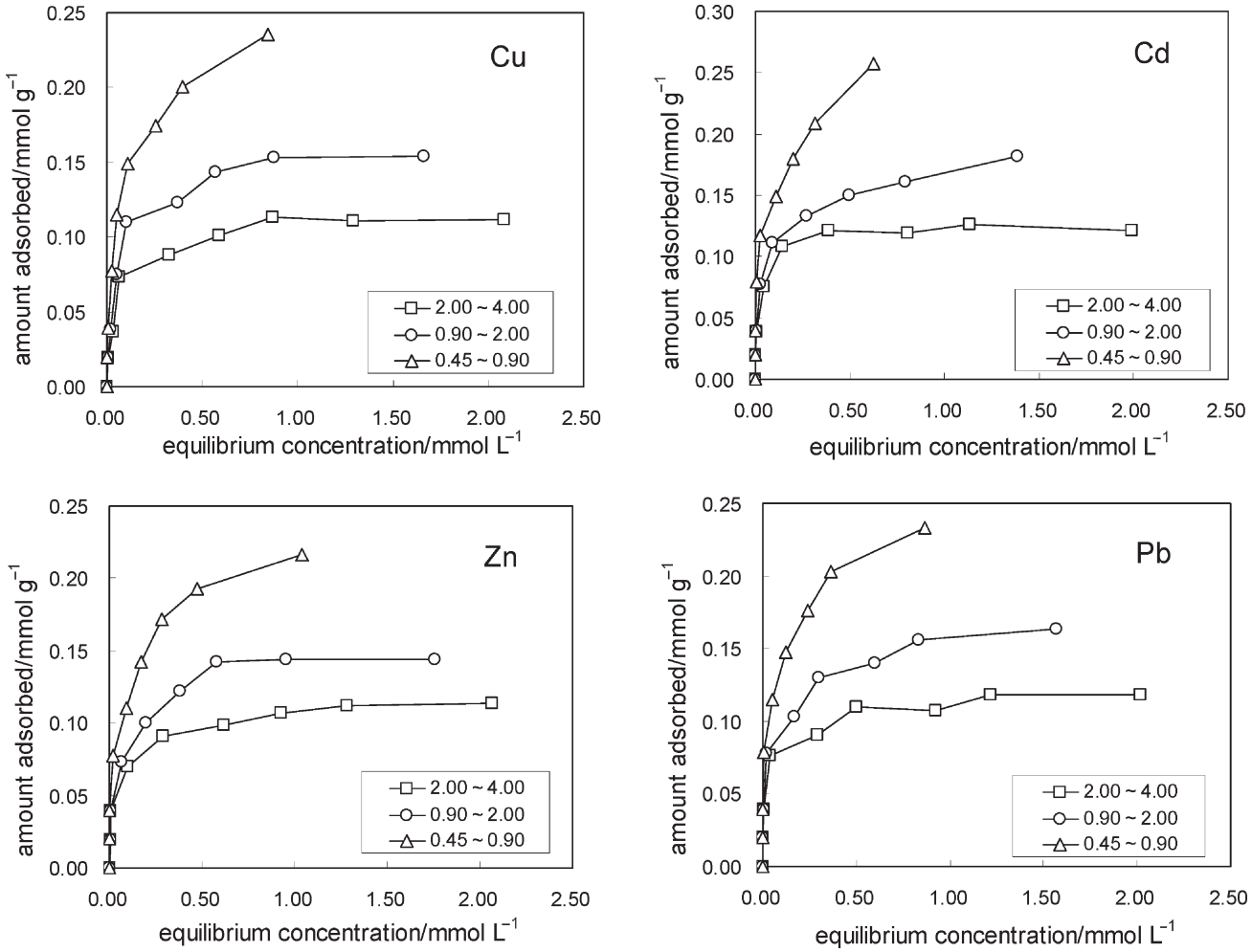

Fig. 8 – *Adsorption isotherms of metal ions on SG slag of different grain size*

correlation coefficients of the two used models revealed that Freundlich model more correctly described the equilibrium of the metal adsorption on SG slag with finer grain size than the Langmuir model. The model of Langmuir isotherm is based on the assumption that the forces of interaction between sorbed molecules are negligible and once a molecule occupies a site, no further sorption takes place, while the Freundlich equation can be described by assuming a heterogeneous surface with adsorption on each class of sites. With the decrease of grain size of SG slag, ion exchange and hydrolysis process would be promoted, resulting in a higher heterogeneity of slag surface. In addition, the adsorption of heavy metal ions of SG slag of finer grain size was prone to follow the Freundlich model.

Conclusion

The present study established that both BS slag and SG slag were effective adsorbents for Cu^{2+}, Cd^{2+}, Zn^{2+} and Pb^{2+} removal from aqueous solutions. The results obtained showed that the adsorption of metal ions on SG slag (0.90~2.00 mm) was higher than that on BS slag (0.90~2.00 mm). The uptake capacities (Q_{max}) for Cu^{2+}, Cd^{2+}, Zn^{2+} and Pb^{2+} adsorption on SG slag (0.90~2.00 mm) were 0.156, 0.166, 0.148, 0.145 mmol g^{-1} respectively, and those for BS slag (0.90~2.00 mm) were 0.101, 0.058, 0.112, 0.120 mmol g^{-1} in the same order of metal ions. However, adsorption kinetics study revealed that the uptake rate of metal ions on BS slag was more rapid, and the metal adsorption on BS slag could achieve pseudo-equilibrium at about 500 min, faster than metal adsorption on SG slag. Adsorption kinetics data of the two EAF slags were well fitted by first-order kinetic model. The data from equilibrium studies confirmed that Freudlich model was better in describing the adsorption of four heavy metal ions on SG slag, while Langmuir model was more applicable for the adsorption on BS slag.

Metal adsorption on the two EAF slags was pH and grain size dependent in aqueous solutions. Moderate increase of initial pH in aqueous solu-

tions could enhance the metal adsorption on the two EAF slags, while initial pH value higher than 7 would restrain the adsorption of Zn^{2+} and Pb^{2+} on the SG slag due to the amphoteric property of metal hydroxide. Batch study data showed that the decrease of grain size of SG slag could increase the uptake capacity of heavy metal ions. However, effects of grain size on the metal removal efficiency in fixed-bed reactor need further research in column experiments, since fine-grain slag can probably cause column clogging, and thus reduce the removal efficiency of metal ions from wastewaters.

ACKNOWLEDGEMENTS

The authors wish to thank the financial support from Key Program of China International Science and Technology Cooperation (2005DFA90960).

List of symbols

q_e – amount of solute adsorbed at equilibrium, mmol g^{-1}

q – amount of solute adsorbed at time t, min

k_1 – rate constant of the first-order adsorption, min^{-1}

k_2 – rate constant of the second-order adsorption, mmol g^{-1} min^{-1}

Q – equilibrium metal concentration on adsorbent, mmol g^{-1}

c_e – equilibrium concentration of metal ions in solution, mmol L^{-1}

K_F – Freundlich adsorption constants

n – Freundlich adsorption constants

Q_{max} – adsoption capacity, mmol g^{-1}

K_L – Langmuir adsorption constant, L $mmol^{-1}$

R^2 – correlation coefficient

Subscripts

EAF – electric arc furnace

SG slag – Shougang slag

BS slag – Baoshan slag

BF – blast furnace

BOF – basic oxygen furnace

XRD – X-ray diffraction

SEM – scanning electron microscopy

AAS – atomic absorption spectrometry

rpm – revolutions per minute

min – minute

References

1. *Zhu, B., Fan, T. X., Zhang, D.,* J. Hazard. Mater. **153** (2008) 300.
2. *Sprynskyy, M., Buszewski, B., Terzyk, A. P., Namiesnik, J.,* J. Colloid Interface Sci. **304** (2006) 21.
3. *Dahiya, S., Tripathi, R. M., Hegde, A. G.,* J. Hazard. Mater. **150** (2008) 376.
4. *Freitas, O. M. M., Martins, R. J. E., Delerue-Matos, C. M., Boaventura, R. A. R.,* J. Hazard. Mater. **153** (2008) 493.
5. *Minamisawa, M., Minamisawa, H., Yoshida, S., Takai, N.,* J. Agric. Food Chem. **52** (2004) 5606.
6. *Chen, J. P., Yu, H.,* J. Environ. Sci. Health, Part A **35** (2000) 817.
7. *Choy, K. K. H., McKay, G.,* Chemosphere **60** (2005) 1141.
8. *Xu, H., Liu, Y.,* Separ. Purif. Technol. **58** (2008) 400.
9. *Wang, S. B., Arivanto, E.,* J. Colloid Interface Sci. **314** (2007) 25.
10. *Moreno, N., Querol, X., Ayora, C., Pereira, C. F., Jurkovicová, M. J.,* Environ. Sci. Technol. **35** (2001) 3526.
11. *Doye, I., Duchesne,* J. Appl. Geochem. **18** (2003) 1197.
12. *Pagnanelli, F., Mainelli, S., De Angelis, S., Toro, L.,* Water Research **39** (2005) 1639.
13. *Vijayaraghavan, K., Jegan, J., Palanivelu, K., Velan, M.,* Chemosphere **60** (2005) 419.
14. *Saeed, A., Iqbal, M.,* Water Research **37** (2003) 3472.
15. *Proctor, D. M., Fehling, K. A., Shay, E. C., Wittenborn, J. L., Green, J. J., Avent, C.,* Environ. Sci. Technol. **34** (2000) 1576.
16. *Cha, W., Kim, J. W., Choi, H. C.,* Water Research **40** (2006) 1034.
17. *Drizo, A., Comeau, Y., Forget, C., Chapuis, R. P.,* Environ. Sci. Technol. **36** (2002) 4642.
18. *Drizo, A., Forget, C., Chapuis, R. P., Comeau, Y.,* Water Research **40** (2006) 1547.
19. *Ramakrishina, K., Viraraghavan, T.,* Waste Manage. **17** (1997) 483.
20. *Dimitrova, S. V., Mehanjiev, D. R.,* Water Research **34** (2000) 1957.
21. *Curkovic, L., Stefanovic, S. C., Mioe, A. R.,* Water Research **35** (2001) 3436.
22. *Ho, Y. S., McKay, G.,* Process Biochem. **34** (1999) 267.
23. *Benguella, B., Benaissa H.,* Water Research **36** (2002) 2463.
24. *Bhattacharyya, K. G., Gupta, S. S.,* J. Colloid Interface Sci. **310** (2007) 411.
25. *Nehrenheim, E., Gustafsson, J. P.,* Bioresour. Technol. **99** (2008) 1571.
26. *Zorpas, A. A., Vassilis, I., Loizidou, M., Grigoropoulou, H.,* J. Colloid Interface Sci. **250** (2002) 1.
27. *Köhler, S. J., Cubillas, P., Blanco, J. D. R., Bauer, C., Prieto, M.,* Environ. Sci. Technol. **41** (2007) 112.
28. *Ouki, S. K., Kavannagh, M.,* Water Sci. Technol. **39** (1999) 115.
29. *Wingenfelder, U., Hansen, C., Furrer, C., Schulin, R.,* Environ. Sci. Technol. **39** (2005) 4606.